Shape transitions between and within Zr isotopes

V. Werner[1,*], *W.* Witt[1], *T.* Beck[1], *N.* Pietralla[1], *M.* Boromiza[2], *C.* Clisu[2], *C.* Costache[2], *I. E.* Dinescu[2], *A.* Ionescu[1], *P. R.* John[1], *P.* Koseoglou[1], *N.* Margineăn[2], *R.* Margineăn[2], *C.* Mihai[2], *R. E.* Mihai[2], *A.* Mitu[2], *A.* Negret[2], *C. R.* Nita[2], *A.* Olacel[2], *S.* Pascu[2], *A.* Serban[2], *C.* Sotty[2], *L.* Stan[2], *R.* Suvaila[2], *S.* Toma[2], *A.* Turturica[2], *S.* Ujeniuc[2], and *J.* Wiederhold[1]

[1]Institut für Kernphysik, Technische Universität Darmstadt, Schlossgartenstr. 9, 64289 Darmstadt, Germany
[2]"Horia Hulubei" National Institute for Physics and Nuclear Engineering, 077125, Bucharest-Magurele, Romania

Abstract. The Zirconium isotopes across the N=56,58 neutron sub-shell closures have been of special interest since years, sparked by the near doubly-magic features of ^{96}Zr and the subsequent rapid onset of collectivity with a deformed ground-state structure already in ^{100}Zr. Recent state-of-the-art shell model approaches did not only correctly describe this shape-phase transition in the Zr isotopic chain, but also the coexistence of non-collective structures and pronounced collectivity especially in ^{96,98}Zr. The isotope ^{98}Zr is located on the transition from spherical to deformed ground state structures. We summarize recent experimental work to obtain the B(E2) excitation strengths of the first 2^+ state of ^{98}Zr, including a new experiment employing the recoil-distance Doppler-shift method following a two-neutron transfer reaction.

1 Introduction

Shape coexistence in nuclei is a well-known phenomenon since decades, but in the last years it has been observed to manifest itself in various forms all across the nuclear chart. Since nuclei are not bound to one specific configuration of nucleons, coupling among themselves in various orbitals (the valence space), they are also not prone to one specific deformation, which is typically given in terms of the classic shape parameters β and γ. Certain microscopic configurations may correspond to different shape parameters. In addition, nuclei in excited states do not necessarily remain within the configuration that they find themselves in their ground states. In turn, already in the ground state, more than one configuration may have significant contribution to the states' total wave function.

With these initial considerations, and restricting to two coexisting shape configurations, two cases of shape coexistence can be classified: first, the case where two differently deformed shapes mix into a given state or sets of states; secondly, the case where certain states or a set of states have distinct shapes. Considering the nuclear potential as a function of deformation, e.g., β deformation, the amount of mixing between different shapes can be ascribed to the interplay of the height of the potential well (barrier) between two potential minima corresponding to different shapes, and of the interaction between both shape configurations (mixing). The two cases are shematically illustrated in Fig. 1, with a spherical potential minimum at $\beta = 0$, and a deformed one at $\beta = \beta_0$. In case of a high barrier in between, sets of eigenstates should exist purely in either configuration. Only if the mixing interaction is strong enough to overcome the barrier, states from both configuration can mix with each other into eigenstates of the system. In the other extreme case, the potential well could be so low, that even with little mixing interaction all eigenstates of the system will be mixtures of both deformations, which become indistinguishable. This is the case, for example, in models such as X(5) [1], where a square well potential is used to approximate the low-barrier situation in Fig. 1, neglecting the small potential barrier between the two minima.

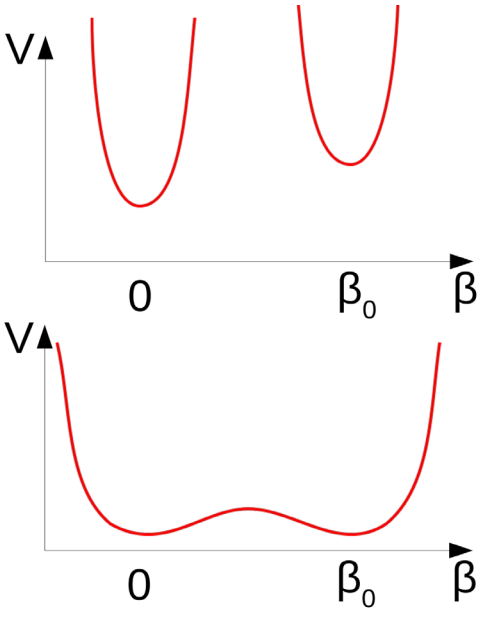

Figure 1. Schematics of nuclear potentials with local minima at β=0 and $\beta = \beta_0$, (top) in case of a high potential barrier and (bottom) in case of a low potential barrier.

*e-mail: vw@ikp.tu-darmstadt.de

The extreme and intermediate cases of the above-mentioned extremes have recently been worked out in Ref. [2]. In the following, we will concentrate on the high-barrier case, where eigenstates are located almost purely in either potential minimum, spherical or deformed. Such a case has recently been identified in ^{96}Zr [3]. In this case a seniority-scheme dominated, non-collective spherical ground state structure exists, coexisting with an excited-state structure which is much more collective and eventually somewhat deformed - the presently available spectroscopic data has recently been summarized in Ref. [4]. This situation has successfully been reproduced within a Monte Carlo shell model (MCSM) approach [5]. The first excited state of ^{96}Zr is located at 1750 keV, with a B(E2) value to the ground state of only 2.3 W.u. [6]. On the contrary, in ^{100}Zr a deformed ground-state structure is known, evident from a low-lying first-2^+ state at 212 keV connected by a strong B(E2) value of 75 W.u. to the ground state [7]. For ^{98}Zr, until recently [8, 9] only the rather high excitation energy of the 2^+_1 state of 1223 keV has been known, but it was not clear whether the assumingly coexisting more collective structure already mixes into its wave function. The latter can be determined from the measurement of its B(E2) transition probability to the ground state. We will summarize the recent experiments to obtain this B(E2) value and present the first estimate from another, complimentary experiment.

2 Recent data on the 2^+_1 state of ^{98}Zr

2.1 Previous works

The B(E2) value of the decay of the 2^+_1 state of ^{98}Zr has recently been constrained by two experiments. In a Coulomb excitation experiment using a radioactive ^{98}Zr beam from Cf fission at Argonne National Laboratory an upper limit for the B(E2) value has been obtained [8], which, combined with a lower limit from a fast-timing experiment [10], constrained the value to 1.83 W.u. $< B(E2; 2^+_1 \rightarrow 0^+_1) <$ 11 W.u., clearly constraining the state to a rather spherical shape, in contrast to the 2^+_1 state of ^{100}Zr with a B(E2) value of 75 W.u.

Another radioactive-beam experiment at GANIL used in-beam U fission reactions to obtain ^{98}Zr and employed the recoil-distance Doppler-shift (RDDS) technique for a direct lifetime measurement [9]. The resulting lifetime further constrained the $B(E2)$ value of interest to 2.9(6)(2) W.u., where the error bars from the measured lifetime and known branching ratio of the state are given separately.

2.2 RDDS after 2n-transfer

We employed another technique to produce ^{98}Zr in its first-excited 2^+ state, namely, a 2-neutron-transfer reaction. A stable ^{18}O beam was delivered at an energy of 49 MeV by the IFIN-HH 9-MV tandem accelerator. The energy was chosen following an excitation function and considering the reaction kinematics, such that recoiling Zr nuclei had maximum momentum in beam direction. The target was a 0.8 mg/cm^2 thick Zr foil, enriched to ^{96}Zr by 57.4 %. The recoiling Zr nuclei were subsequently stopped in an about 10 mg/cm^2 thick Au foil. The distance between both foils was varied using the IFIN plunger device. In this stable-beam experiment the production cross section of ^{98}Zr in the ^{96}Zr(^{18}O,^{16}O)^{98}Zr reaction amounted to less than 10 % of the total cross section, which, even at this sub-Coulomb-barrier energy was dominated by fusion-evaporation reactions. This includes reactions of the beam with the Zr material, but also with oxygen inclusions in the target. Therefore, the measurement suffered from significant background, which forced us to modify the usual RDDS method of measuring the ratio of Doppler-shifted and -unshifted contributions in the spectra. However, in the full spectrum of all distances, the Doppler-shifted components were visible and from their Doppler-shifts an average recoil velocity of v/c = 0.9(1) % was determined, consistent with kinematics calculations.

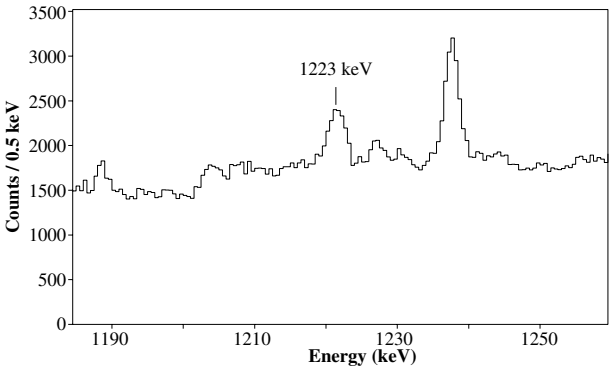

Figure 2. Sum spectrum of the forward-ring detectors, taken at a distance of 74 μm. The stopped peak component from the $2^+_1 \rightarrow 0^+_1$ transition of ^{98}Zr is marked. The Doppler-shifted component is not distinguishable from the background. (From [12].)

The Doppler-shifted peaks from in-flight γ-ray decays of the 2^+_1 state, detected by the ROSPHERE HPGe detector array [11], were too weak and too Doppler-broadened to be distinguished from the background in the individual particle-gated γ-ray spectra for each plunger distance setting and each detector ring (rings at 37°, 90°, and 143° with respect to the beam axis were available). However, the peaks from the stopped component of the decay were visible and, after normalization to other reaction channels, allowed us to obtain a decay curve. A sample spectrum is shown in Fig. 2. Data was taken at an initial three target-to-stopper distances, namely at 25 μm, 74 μm, and 148 μm, where an offset (difference between first electrical contact and actual zero-distance), which has been obtained from extrapolation of the capacitance calibration, is taken into account. After the first three distances the target needed to be cleaned in order to achieve short distances, hence, the distance calibration changed. After realignment another distance setting around 25 μm setting was measured. The offset between the two 25 μm settings was determined from the strong fusion-evaporation reaction producing the 2^+_1 state of ^{110}Cd with a well-known lifetime, resulting in distances of 25 μm and 30 μm, respectively. The use of the known lifetime in ^{110}Cd, hence,

allowed to shift the two parts of the experiment to each other and to obtain a total decay curve. For illustration, the decay curve of the 2_1^+ state of ^{110}Cd is shown in Fig. 3. In addition, the total peak areas from transitions from fusion-evaporation and Coulomb-excitation reactions were used to normalize spectra with respect to the total amount of beam impinging on the target per distance setting.

In addition to the RDDS experiment, data was taken with a 9.2 mg/cm^2 thick ^{96}Zr target from the same material as the RDDS target, in which the recoiling ^{98}Zr nuclei were stopped, hence, minimizing Doppler shift effects. This data was used for a γ-singles and $\gamma\gamma$-coincidence analysis in order to investigate feeding of the 2_1^+ state of ^{98}Zr by other states populated in the 2n-transfer reaction. Only low-spin states (up to spin $J^\pi = 4^+$) were found to be populated. All states which were observed to feed into the 2_1^+ state had either negligible influence on the lifetime of interest from structure-based assumptions made on their lifetimes and feeding intensities, or had known lifetimes which were taken into account in the decay-curve analysis.

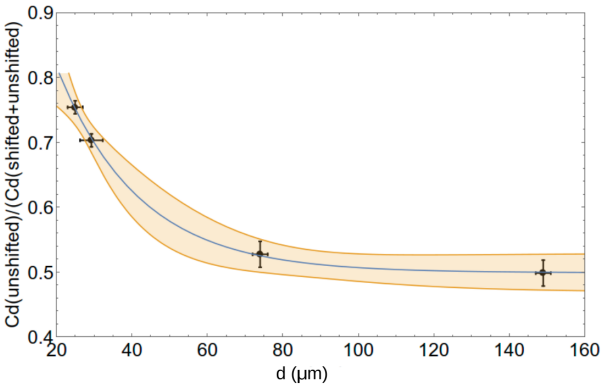

Figure 3. Determination of the distances (especially the 29-μm distance), making use of the known lifetime of the 2_1^+ state of ^{110}Cd. The values for the settings at 25, 74, and 148 μm agree well with the calibrated values, and for the point after realignment of the target 29 μm are obtained. (From [12].)

The full analysis procedure is found in [12] and final results will be given in a forthcoming publication. A preliminary value for the $B(E2; 2_1^+ \rightarrow 0_1^+)$ reduced transition probability, obtained in this RDDS experiment, is 2.8(10) W.u.

3 Discussion

The $B(E2)$ value obtained in the RDDS experiment at IFIN agrees well with the previous limits of Refs. [8, 10], as well as the $B(E2)$ value obtained in Ref. [9] of 2.9(6)(2) W.u., having a similar combined uncertainty. Therefore, in the following we will use the average value of the present work and [9] of 2.8(6) W.u. This value is incorporated into the systematics shown in Fig. 4, showing the energy differences of first and second 0^+ and 2^+ states, and the $B(E2; 2_1^+ \rightarrow 0_1^+)$ values over the relevant Zr isotopes. Firstly, the new $B(E2)$ value for ^{98}Zr is at the lower edge of the pervious limiting values, and clearly shows a non-collective excitation of the 2_1^+ state, similar to the lighter Zr isotopes, and in stark contrast to ^{100,102}Zr, where the transition is strongly collective (see Fig. 4). Secondly, the systematics of energy differences reveal that, considering a two-level crossing scenario, the 2^+ states are closest already in ^{98}Zr, whereas the 0^+ states are closest in ^{100}Zr, as shown in the bottom panel of Fig. 4. This means that the crossing of weakly and strongly collective structures occurs at smaller N for the 2^+ states, and the 2_1^+ state of ^{98}Zr could, in fact, be the state that belongs to the collective structure. The latter is corroborated by the strong $B(E2; 2_1^+ \rightarrow 0_2^+)$ transition of 28(6) W.u. (using the average of this work and Ref. [9]). Hence, the ground state of ^{98}Zr is the non-collective counterpart of the ground states of the lighter Zr isotopes, and the first excited 0_2^+ state has significant collectivity, with the 2_1^+ state built on it as a collective excitation.

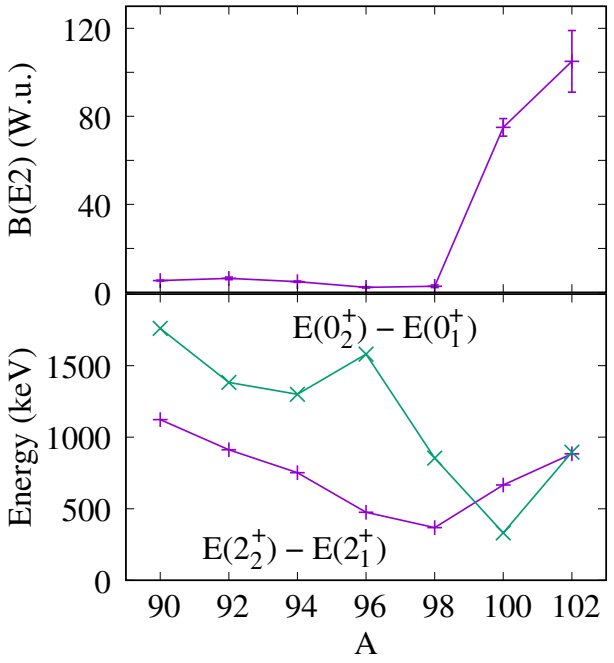

Figure 4. Top panel: Evolution of the $B(E2)$ values from the first 2^+ state over the Zr isotopic chain over mass number A. Bottom panel: Energy differences between the $0_{1,2}^+$ states and between the $2_{1,2}^+$ states in the Zr isotopes.

However, the $B(E2)$ value of 28 W.u. within the excited, collective structure of ^{98}Zr does not quite match the collectivity of the ground-state structure of ^{100}Zr with a corresponding $B(E2)$ value of 75 W.u. This observation triggers the idea that the collective structure itself may undergo an evolution across ^{98}Zr, while it becomes the ground-state structure, presumably changing place in energy with the non-collective structure. It is, however, an open question whether the non-collective structure actually survives in ^{100}Zr, or whether it starts mixing with other configuration and therefore looses the distinct signatures that it has up to ^{98}Zr.

This scenario has recently been theoretically fleshed out by Gavrielov, Leviatan and Iachello [13] within an al-

gebraic approach. The finding of their work was the occurrence of an intertwined phase transition in the Zr isotopes, meaning the simultaneous occurrence of two quantum phase transitions. Firstly, two distinct and weakly mixing configurations exist - a non-collective one based on the closures of proton ($N = 40$) and neutron ($N = 50, 56$) (sub)-shells, and the other a collective configuration which in the framework of Ref. [13] starts as a spherical vibrator [U(5) in terms of the algebraic model]. A type-II phase transition occurs as the non-collective and the collective structures exchange place in energy, without substantial mixing, which corresponds to the high-barrier case sketched in Fig. 1. Moreover, due to the different energy spacings between levels within the respective configurations, the first excited 2^+ states already crossed in ^{98}Zr, whereas the lowest, i.e., the 0^+ states of the respective configurations exchanged position in ^{100}Zr. This is evident from the collective $B(E2; 2_1^+ \rightarrow 0_2^+)$ value in ^{98}Zr, whereas there is little overlap between the two configuration, witnessed by the weak observed $B(E2; 2_1^+ \rightarrow 0_1^+)$ value in this isotope.

However, a structural change within the collective structure is observed across $N = 60$. In the framework of Ref. [13] this change is described as a type-I phase transition, i.e., a quantum phase transition within the valence space given for this configuration. From the observed $B(E2)$ values the ground-state configurations of ^{100,102}Zr with substantial $B(E2)$ values should be well-deformed, hence, the transition is from the vibrational U(5) limit to the well-deformed rotor limit SU(3). This particular transition corresponds to the low-barrier case depicted in Fig. 1, which is a soft potential on the transition from a spherical-centered vibrational case and a potential with a distinct minimum at a given deformation value β_0, corresponding to the approximation of the X(5) model.

4 Conclusions

We performed a RDDS lifetime measurement on the first excited 2^+ state of ^{98}Zr. Our results are in good agreement with recent experiments. The data strongly supports the recently established picture of a intertwined quantum phase transition in the Zr isotopes across $N = 60$. A non-collective spherical structure exchanges with a collective ("intruder") structure at ^{98,100}Zr through a type-II phase transition, while simultaneously the intruder structure undergoes a type-I phase transition from presumably a spherical vibrator to a axially-deformed rotor. To further disentangle collective and non-collective structures in ^{98}Zr larger sets of electro-magnetic matrix elements among its low-lying states, are needed, especially for the lowest 2^+ states, e.g., from high-statistics multi-step Coulomb-excitation data.

Acknowledgments

We thank A. Leviatan, N. Gavrielov and F. Iachello for many discussions on the topic of quantum phase transitions in the Zr isotopes. Further, we thank the crew of the IFIN tandem accelerator for excellent beam conditions. This work was supported by German BMBF und grant no. 05P19RDFN1 and DFG grant SFB 1245, and by the Romanian MCI Project PN 19 06 01 02.

References

[1] F. Iachello, Phys. Rev. Lett. **87**, 052502 (2001).
[2] R. Budaca and A. I. Budaca, Eur. Phys. Lett. **123**, 42001 (2018).
[3] C. Kremer, S. Aslanidou, S. Bassauer, M. Hilcker, A. Krugmann *et al.*, Phys. Rev. Lett. **117**, 172503 (2016).
[4] W. Witt, N. Pietralla, V. Werner, and T. Beck, Eur. Phys. J. A **55**, 79 (2019).
[5] T. Togashi, Y. Tsunoda, T. Otsuka, and N. Shimizu, Phys. Rev. Lett. **117**, 172502 (2016).
[6] G. Kumbartzki, N. Benczer-Koller, J. Holden, G. Jakob, T.J. Mertzimekis *et al.*, Phys. Lett. B **562**, 193 (2003).
[7] B. Singh, Nucl. Data Sheets **109**, 297 (2008).
[8] W. Witt, V. Werner, N. Pietralla, M. Albers, A. D. Ayangeakaa *et al.*, Phys. Rev. C **98**, 041302(R) (2018).
[9] P. Singh, W. Korten, T. W. Hagen, A. Görgen, L. Grente *et al.*, Phys. Rev. Lett. **121**, 192501 (2018).
[10] S. Ansari, J.-M. Régis, J. Jolie, N. Saed-Samii, N. Warr *et al.*, Phys. Rev. C **96**, 054323 (2017).
[11] D. Bucurescu, I. Căta-Danil, G. Ciocan, C. Costache, D. Deleanu *et al.*, Nucl. Instrum. Methods A **837**, 1 (2016).
[12] W. Witt, Dissertation, TU Darmstadt, 2019.
[13] N. Gavrielov, A. Leviatan, and F. Iachello, Phys. Rev. C **99**, 064324 (2019).